DOI: 10.1002/cssc.201402087

Simulated Performance of Reactor Configurations for Hot-Water Pretreatment of Sugarcane Bagasse

Véronique Archambault-Léger,[a, b] Xiongjun Shao,[a, b] and Lee R. Lynd*[a, b, c]

During the pretreatment of cellulosic biomass for subsequent microbial or enzymatic processing, the fiber reactivity typically increases with increasing severity but so does sugar degradation. Experimental results with sugarcane bagasse show that this tradeoff can be mitigated substantially by pretreatment in a flow-through (FT) mode. A model that incorporates both kinetics and mass transfer was developed to simulate the performance of pretreatment in plug flow, counter-current flow, cross flow, discrete counter-current and partial FT configurations. The simulated results compare well to the literature for bagasse pretreated in both batch and FT configurations. A variety of FT configurations result in sugar degradation that is very low (1–5%) and 5–20-fold less than a conventional plug flow configuration. The performance exhibits strong sensitivity to the extent of hemicellulose solubilization, particularly for a conventional plug flow configuration.

Introduction

The production of fuel from lignocellulosic biomass is of interest in the context of the development of a sustainable global energy system.[1] The main obstacle that impedes the production of cost-competitive cellulosic biofuels is the high cost of the conversion of cellulosic feedstocks to reactive intermediates, termed biomass recalcitrance. In the case of the biological conversion of cellulosic biomass to sugars, recalcitrance results from the incomplete accessibility of attack by microbes and their saccharolytic enzymes because of structural features, heterogeneous composition, and chemical linkages between the components.[2]

In the biomass conversion field, "pretreatment" refers to the process that converts cellulosic biomass into a form amenable to biological attack. Various pretreatment approaches allow subsequent enzymatic hydrolysis yields of 90% or more, whereas low yields have been observed widely in the absence of pretreatment.[3] Pretreatment processes examined in the literature include exposure to acid or alkali, ammonia, lime, organic solvents, ionic liquids, steam explosion, and water, generally at elevated temperature and pressure.[3,4] Pretreatment has multiple objectives that are challenging to achieve at once. In particular, high cellulose reactivity is fostered by reaction at high temperature and long reaction times, yet such conditions result commonly in the degradation of sugars and the production of fermentation inhibitors from hemicellulose.

Solubilized sugars have less time to degrade if a flow-through (FT) configuration is used as the liquid is removed from the reactor. In addition, recondensation of solubilized lignin and hemicellulose on cellulose fibers upon cooling occurs to a lesser extent in an FT configuration compared to configurations without FT.[5] Consistent with this understanding, FT pretreatment typically achieves higher solids reactivity, higher hemicellulose removal, less sugar degradation, and substantially higher removal of lignin compared to pretreatment in non-FT configurations at the same temperature and residence time.[3–5] Previous studies have found that the mass ratio of liquid to solids,[6] particle size,[7] and flow velocity[8] have an impact on pretreatment performance, however, the impact of dilution may not be significant below a solids concentration of 10 w/v%.

Many kinetic models have been reported that describe the kinetics of pretreatment using hot water[9] or dilute acid.[10] Most of these considered the reactions involved in hemicellulose hydrolysis and degradation. For hydrothermal pretreatment, it has been shown that hemicellulose is solubilized to oligomers that form degradation products directly with monomeric sugars only produced at low levels.[9b,11] The effect of mass transfer has been studied in both batch and FT reactors.[12] Cross flow has also been considered in an annular reactor.[13]

The operation of FT configurations in a practical context is challenging because the higher water usage compared to non-FT configuration dilutes the sugar streams and increases energy consumption.[14] Several configurations have been proposed and investigated to address these concerns, which include recirculation flow, partial flow, and counter-current flow. Recirculation controls the dilution and energy consumption but fails to realize many of the benefits of other FT configura-

[a] Dr. V. Archambault-Léger, Prof. Dr. X. Shao, Prof. Dr. L. R. Lynd
Dartmouth College
Hanover NH 03755 (USA)
E-mail: Lee.R.Lynd@Dartmouth.edu

[b] Dr. V. Archambault-Léger, Prof. Dr. X. Shao, Prof. Dr. L. R. Lynd
DOE BioEnergy Science Center
Oak Ridge National Laboratory
Oak Ridge TN 37831 (USA)

[c] Prof. Dr. L. R. Lynd
Mascoma Corporation
Lebanon NH 03766

Supporting Information for this article is available on the WWW under http://dx.doi.org/10.1002/cssc.201402087.

tions.[14] Partial flow was shown to increase sugar and lignin removal and to yield more reactive fibers compared to batch operation.[15] Modeling suggests that counter-current flow could produce a higher concentration of solubilized sugar and less sugar degradation as compared to more conventional configurations.[9a]

Although continuous counter-current flow operation is common in the wood pulp and paper industry[16] and has been reported for wheat straw pretreatment at a pilot scale,[17] the operation of continuous full reactor FT pretreatment at scale is challenging[18] in general and in particular for sugarcane bagasse. The mechanical properties of bagasse cause channeling, compacting, and a very high resistance to flow.[19] Therefore, partial flow, which combines FT and non-FT reactor sections,[15] may be a more practical configuration. Partial flow has the potential to be studied further, and optimization of the pretreatment configuration combinations may realize the advantages of FT and minimize sugar dilution and energy consumption. The evaluation of a variety of reactor configurations within a common framework that includes both kinetics and mass transfer has not been reported previously.

In the present study, we develop a kinetic and mass transfer model to predict hemicellulose solubilization and degradation for sugarcane bagasse in batch and FT configurations and use this model to investigate hemicellulose profiles and solid fibers reactivity for several reactor configurations.

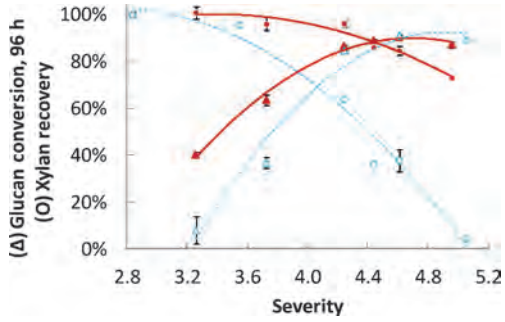

Figure 1. Glucan conversion (triangles) and hemicellulose recovery (circles) as a function of severity for different pretreatment configurations for sugarcane bagasse. Open symbols and dotted lines: batch. Closed symbols and solid lines: FT. The error bars show the standard deviation of duplicate measurements.

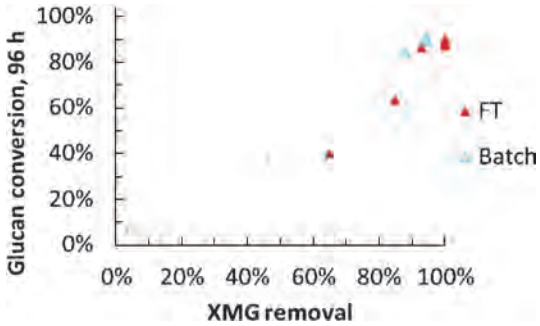

Figure 2. Glucan conversion after 96 h of enzymatic hydrolysis against XMG removal after FT- and batch-pretreated bagasse.

a) Models 1 and 3: Reaction only

$$\frac{\partial H}{\partial t} = v\frac{\partial H}{\partial Z} + H\left(\frac{\partial v}{\partial Z} - k1\right)$$

$$\frac{\partial O}{\partial t} = u\frac{\partial O}{\partial Z} + k1 * H - k2 * O$$

$$\frac{\partial DP}{\partial t} = u\frac{\partial DP}{\partial Z} + k2 * O$$

b) Models 2 and 4: Reaction and mass transfer

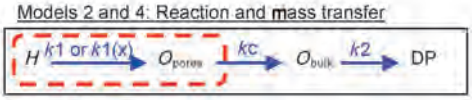

$$\frac{\partial H}{\partial t} = v\frac{\partial H}{\partial Z} + H\left(\frac{\partial v}{\partial Z} - k1\right)$$

$$\frac{\partial O_{pores}}{\partial t} = v\frac{\partial O_{pores}}{\partial Z} + O_{pores}\frac{\partial v}{\partial Z} + k1 * H - kc * A\left(\frac{O_{pores}}{V} - \frac{O_{bulk}}{U}\right)$$

$$\frac{\partial O_{bulk}}{\partial t} = u\frac{\partial O_{bulk}}{\partial Z} + kc * A\left(\frac{O_{pores}}{V} - \frac{O_{bulk}}{U}\right) - k2 * O_{bulk}$$

$$\frac{\partial DP}{\partial t} = u\frac{\partial DP}{\partial Z} + k2 * O$$

c) Model 5: Reaction and mass transfer with degradation inside pores

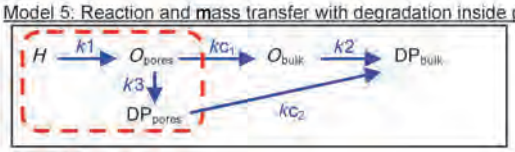

$$\frac{\partial H}{\partial t} = v\frac{\partial H}{\partial Z} + H\left(\frac{\partial v}{\partial Z} - k1\right)$$

$$\frac{\partial O_{pores}}{\partial t} = v\frac{\partial O_{pores}}{\partial Z} + O_{pores}\frac{\partial v}{\partial Z} + k1 * H - k3 * O_{pores} - kc_1 * A\left(\frac{O_{pores}}{V} - \frac{O_{bulk}}{U}\right)$$

$$\frac{\partial DP_{pores}}{\partial t} = v\frac{\partial DP_{pores}}{\partial Z} + DP_{pores}\frac{\partial v}{\partial Z} + k3 * O_{pores} - kc_2 * A\left(\frac{DP_{pores}}{V} - \frac{DP_{bulk}}{U}\right)$$

$$\frac{\partial O_{bulk}}{\partial t} = u\frac{\partial O_{bulk}}{\partial Z} + kc_1 * A\left(\frac{O_{pores}}{V} - \frac{O_{bulk}}{U}\right) - k2 * O_{bulk}$$

$$\frac{\partial DP_{bulk}}{\partial t} = u\frac{\partial DP_{bulk}}{\partial Z} + k2 * O_{bulk} + kc_2 * A\left(\frac{DP_{pores}}{V} - \frac{DP_{bulk}}{U}\right)$$

d) Cross Flow configuration equations for Model 2

$$\frac{\partial H}{\partial t} = v\frac{\partial H}{\partial Z} + H\left(\frac{\partial v}{\partial Z} - k1\right)$$

$$\frac{\partial O_{pores}}{\partial t} = v\frac{\partial O_{pores}}{\partial Z} + O_{pores}\frac{\partial v}{\partial Z} + k1 * H - kc * A\left(\frac{O_{pores}}{V} - \frac{O_{bulk}}{U}\right)$$

$$\frac{\partial O_{bulk,axial}}{\partial t} = v\frac{dO_{axial}}{dZ} + kc * A\left(\frac{O_{pores}}{V} - \frac{O_{bulk}}{U}\right) - k2 * O_{axial} - \frac{O_{axial}}{U}\frac{\partial V_{SS}}{\partial Z}$$

$$\frac{\partial DP_{axial}}{\partial t} = v\frac{\partial DP_{axial}}{\partial Z} + k2 * O_{axial} - \frac{DP_{axial}}{v * U}\frac{\partial V_{SS}}{\partial Z}$$

$$\frac{\partial O_{bulk,ss}}{\partial t} = v\frac{\partial O_{bulk,ss}}{\partial Z} + \frac{O_{bulk,axial}}{v * U}\frac{\partial V_{SS}}{\partial Z}$$

$$\frac{\partial DP_{ss}}{\partial t} = v\frac{\partial DP_{ss}}{\partial Z} + \frac{DP_{axial}}{v * U}\frac{\partial V_{SS}}{\partial Z}$$

Figure 3. Kinetic equations for a) models 1 and 3 (reaction only), b) models 2 and 4 (reaction and mass transfer), c) model 5 (reaction and mass transfer model with degradation within pores), and d) cross flow configuration.

Results and Discussion

Batch and FT pretreatment comparison

Pretreatment has multiple objectives that are challenging to achieve at once. In particular, high cellulose reactivity is fostered by reaction at high temperature and long reaction times, yet such conditions commonly result in the degradation of sugars and production of fermentation inhibitors. To assess cellulose reactivity, simultaneous saccharification and fermentation (SSF) with a protein loading of 10 FPU g_{glucan}^{-1} (6 $mg_{protein}\,g_{glucan}^{-1}$) and an initial substrate concentration of 20 $g_{glucan}\,L^{-1}$ was performed following a method described previously[20] on pretreated bagasse. FT pretreatment of sugarcane bagasse has the potential to achieve both high cellulose reactivity and low hemicellulose degradation under one set of reaction conditions (Figure 1). Severity (R_o) is defined as shown in Equation (1):[21]

$$R_o = t \cdot \exp[(T-100)/14.75)] \quad (1)$$

in which t is the time of reaction [min] and T is the temperature of the reaction [°C]. Conditions severe enough to enable 90% glucan conversion during enzymatic hydrolysis decrease the cumulative recovery of xylan, mannan, and galactan (XMG) to ≈50% for batch pretreatment, whereas XMG recovery is ≈85% for FT pretreatment.

High enzymatic hydrolysis is fostered by greater than ≈90–95% XMG removal for both batch and FT pretreatments (Figure 2). Yang and Wyman[22] showed a similar linear trend between glucan conversion after enzymatic hydrolysis and hemicellulose removal with corn stover.

Model development

Five types of kinetic models were fitted to experimental data by using Berkeley Madonna software for sugarcane bagasse and compared. Model 1, illustrated in Figure 3a along with its partial differential equations, consists of a series of two first-order kinetic reactions in which hemicellulose (H) is hydrolyzed to oligomers (O) and reacted directly to degradation products (DP). Model 2 (Figure 3b) was proposed by Brennan[12a] and incorporates mass transfer. The soluble hemicellulose is first contained in the pores (O_{pores}) of the solid fibers before it is transported to the bulk solution (O_{bulk}) and then reacted to form degradation products. Both models were studied with the hemicellulose kinetic parameter constant ($k1$, Models 1 and 2) and conversion-dependent ($k1(x)=(1-x)^m$, Models 3 and 4), which was suggested by Shao and Lynd.[9a] Model 5 considers degradation within the pores of the solids as well as in the bulk solution as described in Figure 3c. To model a cross flow configuration, additional terms that describe the accumulation of oligomers ($O_{bulk,ss}$) and degradation products (DP_{ss}) were added. The side stream accumulation term is also subtracted from the axial partial differential equations. An example of these additional terms using Model 2 is shown in Figure 3d.

Data fitting

Models 1–5 described in the previous section were fitted to bagasse batch and FT pretreatment data (Figure 4). The batch data were taken from Jacobsen's work,[12b] and the FT pretreatment data were collected for the present study using methods described previously.[20] Model 5 considers oligomer degradation within the pores and led to a negative value of the additional kinetic parameter $k3$. This model was rejected as the degradation reaction is irreversible and a negative $k3$ is not physically meaningful. Model 2, which incorporates reactions and mass transfer, provides the best fit for both batch and FT data and predicts both batch and FT experimental data well with an adjusted coefficient of determination of 0.90 and 0.93, respectively (Table 1). This model was thus chosen to investigate several configurations.

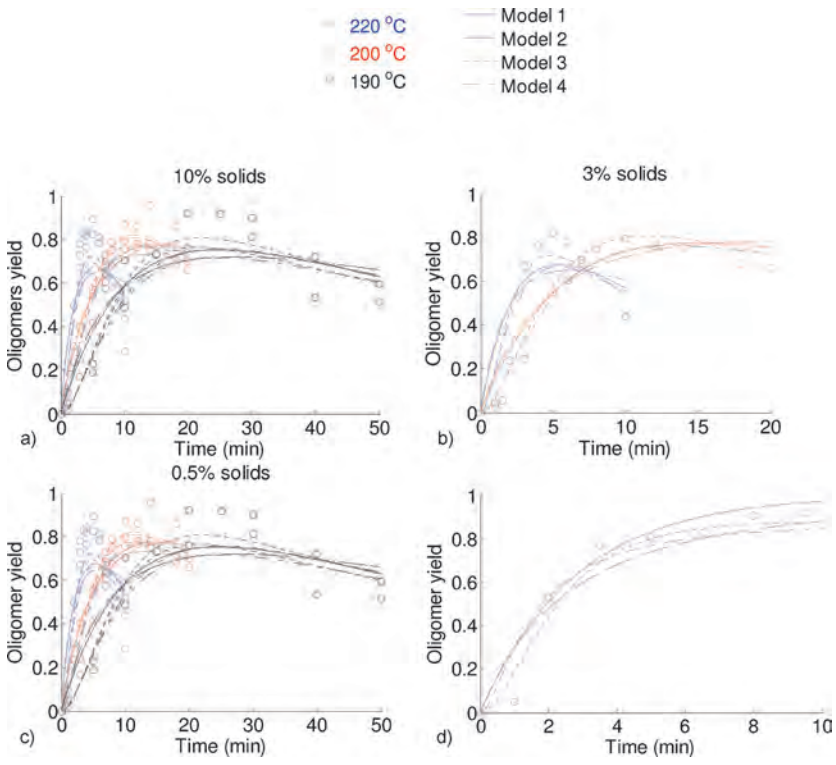

Figure 4. Bagasse data parameter fitting: a) batch 10% solids, b) batch 3% solids, c) batch 0.5% solids,[12b] and d) FT (30 $mL\,min^{-1}$).

Table 1. Adjusted R^2 for Models 1–4 fitted to batch and FT pretreatment data.

Model	Parameter	Adjusted R^2 batch data	FT data
1	reaction only, constant $k1$	0.82	0.89
2	reaction and mass transfer, constant $k1$	0.90	0.93
3	reaction only, conversion-dependent $k1(x)$	0.77	0.84
4	reaction and mass transfer, conversion-dependent $k1(x)$	0.86	0.81

Configurations evaluated

We examined the performance of several configurations for the continuous processing of biomass that combine FT and non-FT sections. The configurations studied were a) plug flow, b) counter-current flow (CC), c) discrete counter-current, d) cross flow, e) sequential plug and cross flow (SPC), f) sequential plug and counter-current flow (SPCC), and g) sequential plug and co-current flow (SPCo; Figure 5).

Configuration optimization

Configurations a)–g) were modeled by using matlab with a temperature gradient from the solids inlet to the solids outlet. The temperature gradient and the solids residence time were optimized for each configuration studied to obtain the highest possible fraction of initial hemicellulose recovered in the liquid. All configurations were constrained to 1) remove 90.0±0.05 and 95.0±0.05% hemicellulose from the solids to provide highly digestible fibers and 2) give an overall mass ratio of liquid to solids ($R_{l/s}$) of 6.0±0.1, which is relevant in a practical context.[23] If we assume a bagasse density of 1500 kg m^{-3},[24] the reactor void volume was 0.9. In partial FT configurations, the void volume in non-flow regions was ≈0.85–0.87 to ensure the absence of flow in those regions. A cross flow configuration achieves a very high recovery of hemicellulose in the liquid and very little hemicellulose degradation at the expense of high dilution. As $R_{l/s}$ could not be kept as low as 6, complete cross flow optimization is not reported here.

If 90% of the hemicellulose was removed from the solids, 68–78% was recovered in the liquid phase for plug flow. The hemicellulose recovery was maximized with a temperature gradient of 135–180 °C and a solids residence time of 59 min. The residence time can be reduced to ≈25 min with a 5% loss in hemicellulose recovered in the liquid phase by increasing the temperature to 200 °C (Figure 6a). If the optimization is constrained to 95% hemicellulose removal, the hemicellulose degradation increases drastically because the additional 5% removal occurs at the end of the reactor at which the solubilized compounds are already concentrated. The response surface in this situation is flat (±1%), and the high temperatures (210–225 °C) required to remove 95% of the hemicellulose from the solids result in 47–49% hemicellulose degradation. This is consistent with the results shown in Figure 1, which indicates that conditions sufficient to yield highly digestible fibers result in

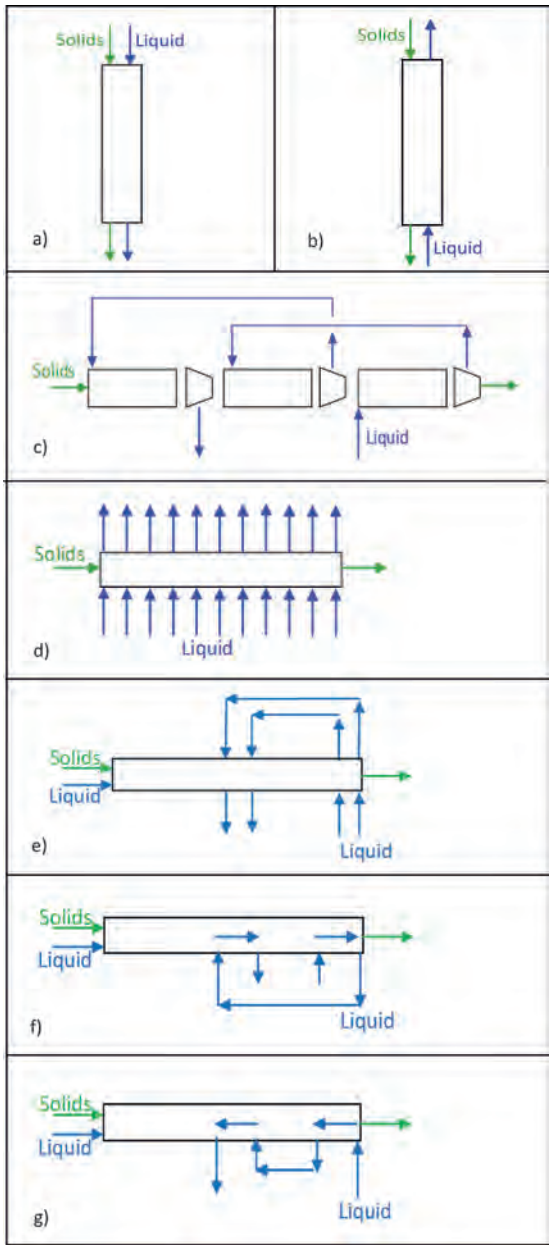

Figure 5. Reactor configurations of interest: a) plug flow, b) counter-current (CC), c) discrete counter-current, d) cross flow, e) sequential plug and cross flow (SPC), f) sequential plug and counter-current flow (SPCC), and g) sequential plug and co-current flow (SPCo).

≈50% XMG degradation. Although 95% hemicellulose removal may give more digestible fibers than 90% removal, it is not desirable to achieve this additional removal by using plug flow because of the 25–37% increase in sugar degradation.

For CC, the hemicellulose recovered in the liquid phase if 90% is removed from the solids varied between 84 and 88% and was maximized with a temperature gradient of 135–180 °C and a liquid residence time of 59 min. The residence time can be reduced to ≈25 min with less than 2% loss in hemicellulose recovered in the liquid phase by increasing the temperature to 205 °C (Figure 6b). The upper right corner of Figure 6a is not relevant because the high temperature and long resi-

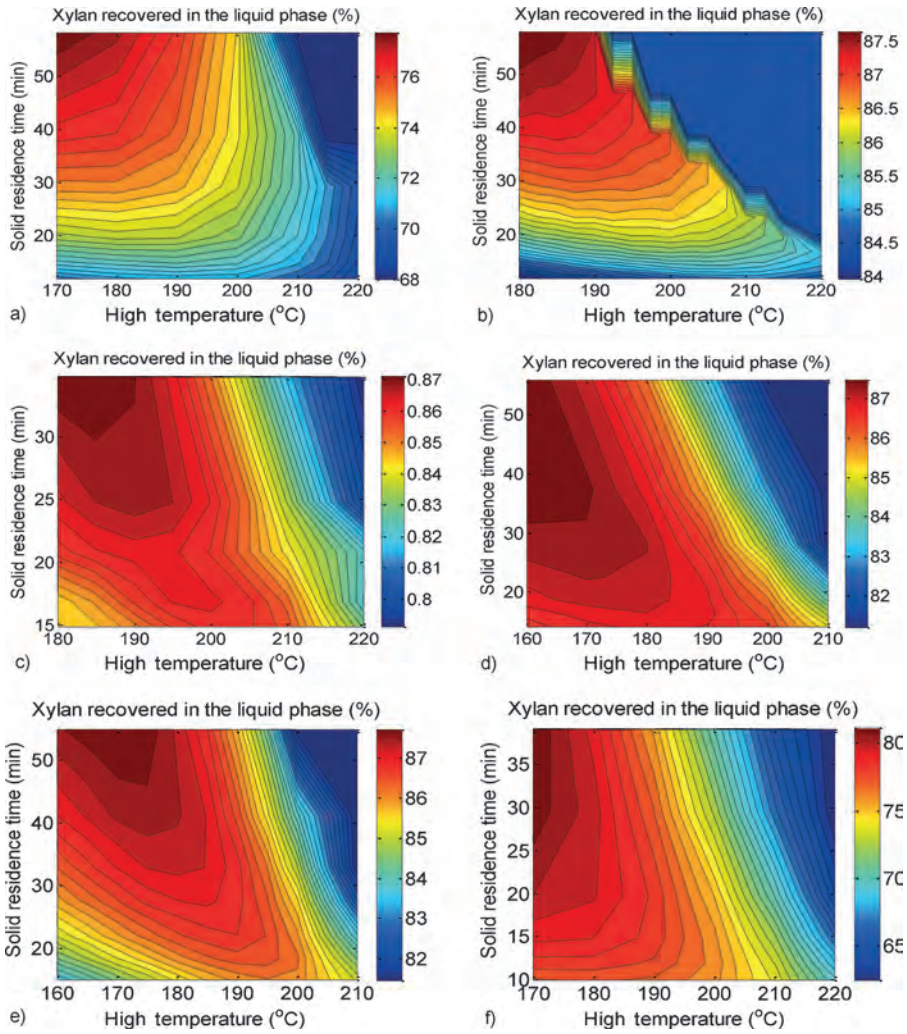

Figure 6. Percentage of initial hemicellulose recovered in the liquid phase as a function of solids residence time and temperature if 90% of the hemicellulose is removed from the solids. a) Plug flow, b) Cc, c) SPC, d) SPCC, e) SPCo, and f) discrete cc (two stages).

dence time would require a temperature at the solids entrance of less than 100 °C, below which the pretreatment reaction is negligible and the model cannot predict results reliably. If the optimization was constrained to 95% hemicellulose removal, hemicellulose degradation increased by less than 1%, whereas the hemicellulose recovery in the liquid increases by more than 4% because the additional 5% removal occurs at the end of the reactor at which new water enters at the highest temperature in the reactor. The FT data shown in Figure 4d agree with these predictions and give ≈90% oligomer yield after 10 min at 220 °C. Similar to CC, the hemicellulose recovery for SPC, SPCC, and SPCo configurations is maximized at a high residence time and low temperature, but a decrease of the residence time and increase of the temperature has only a small penalty (Figure 6).

The performance of two- and three-stage discrete counter-current configurations lay between that of FT and non-FT configurations. The dewatering units cannot remove all the water in the reactor and it was assumed, based on diffuser dewatering capacities, that they could dewater bagasse down to 50% moisture. The optimal condition for two stages and 90% removal gave 81.7% hemicellulose recovery and 8.3% degradation. Three stages improved these values by less than 1%. If the optimization was constrained to 95% hemicellulose removal, hemicellulose degradation increased by 4%, whereas the hemicellulose recovery in the liquid increased by only 1%. In addition to the kinetic model that indicates the lower performance of discrete counter-current configuration than FT configurations, dewatering units are very expensive. Thus the discrete counter-current configuration is not considered to be a promising option.

The percentage of initial hemicellulose recovered in the liquid and degraded for plug flow, CC, discrete counter-current, SPC, SPCC, and SPCo configurations under the optimized conditions are summarized in Table 2. Up to 87.4–92.5% of the initial hemicellulose is recovered in the liquid phase for flow configurations compared with 46.9–78.1% for the plug flow configuration. Clearly, flow configurations can provide higher sugar recovery than plug flow under conditions that give highly reac-

Table 2. Comparison of maximum oligomer yield and associated degradation yield for plug-flow, counter-current, and partial-flow configurations for 90% and >95% hemicellulose removal.

Configuration	Initial hemicellulose recovered in liquid [%]		Initial hemicellulose degraded [%]	
	90%	>95%	90%	>95%
plug flow	78.1<	>46.9	11.6<	>48.1
counter-current (CC)	87.8<	>92.4	2.0<	>2.6
discrete counter-current (two stages)	81.7<	>82.5	8.3<	>12.5
discrete counter-current (three stages)	82.4<	>83.1	7.6<	>12.0
partial flow: sequential plug and cross flow (SPC)	87.4<	>90.5	2.5<	>4.5
partial flow: sequential plug and counter-current flow (SPCC)	87.7<	>92.3	1.6<	>2.7
partial flow: sequential plug and co-current flow (SPCo)	87.9<	>91.3	2.1<	>3.6

tive fibers. All flow configurations studied can be optimized to give 1.6–4.5% hemicellulose degradation. These results suggest several flow-type options for a high-performance pretreatment reactor. The most practical option should be chosen based on factors not considered in the current kinetic study, which include mechanical feasibility, sugar dilution, and energy consumption.

Analysis of configurations of interest

Hemicellulose recovery and degradation profiles as a function of the fractional progress of the liquid in the reactor (Z) for plug flow, CC, and partial FT configurations that use the optimized conditions described in the previous section and 90% hemicellulose removal are presented in Figure 7. SPC removes the oligomers where they are most concentrated to result in 87.4% of initial hemicellulose recovered in the liquid and 2.5% hemicellulose degradation (Figure 7a). SPCC achieves 87.7% hemicellulose recovery in the liquid and 1.6% hemicellulose degradation (Figure 7b). SPCo achieves 87.9% hemicellulose recovery in the liquid and 2.1% hemicellulose degradation (Figure 7c).

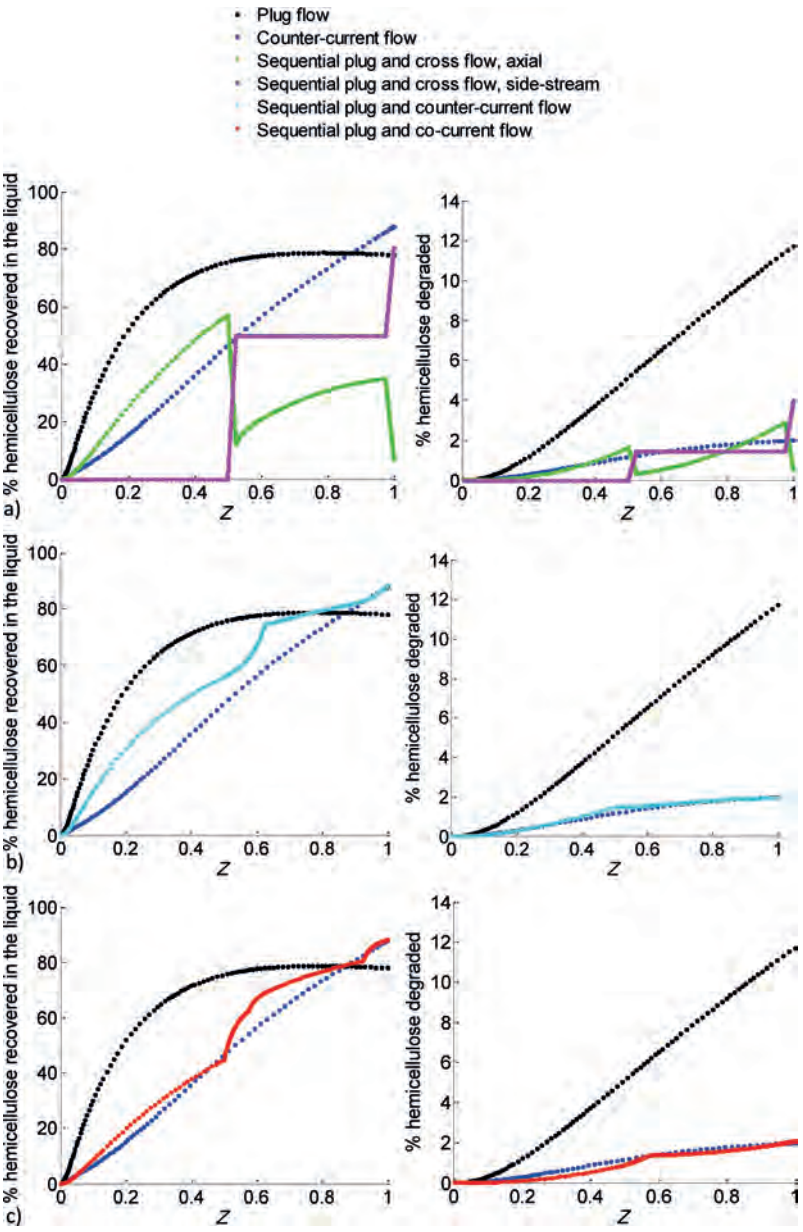

Figure 7. Yield of solubilized hemicellulose (left) and degradation products (right) against the fractional progress of the liquid (Z) in the reactor using reaction and mass transfer model for plug flow counter-current and a) sequential plug and cross flow (SPC), b) sequential plug and counter-current (SPCC) flow, and c) Sequential plug and co-current (SPCo) flow.

Conclusions

A kinetic and mass transfer model was developed that predicted both batch and flow-through (FT) experimental data well. Under reaction conditions that give high enzymatic hydrolysis, 87.4–92.5% of the initial hemicellulose is recovered in the liquid phase for flow configurations compared with 46.9–78.1% for the plug flow configuration. Flow configurations result in 1–5% hemicellulose degradation, a 5–20-fold reduction compared to plug flow. Partial FT pretreatment that incorporates plug flow and flow regions could provide highly digestible solid fibers and high sugar recovery under one set of reaction conditions, be more mechanically practical than complete counter-current flow, and help to address sugar dilution and energy consumption challenges.

Glossary

A	Specific surface area of the solid particles [dm g^{-1}]
CC	Counter-current flow
DP	Flow rate of degradation products [g min^{-1}]
DP_{axial}	Axial flow rate of degradation products [g min^{-1}]
DP_{ss}	Accumulation of degradation products in side stream [g min^{-1}]
FT	Flow-through
H	Flow rate of hemicellulose [g min^{-1}]
$k1$	Kinetic parameter of hemicellulose [min^{-1}]

$k2$	Kinetic parameter of oligomers [min^{-1}]
kc	Mass transfer coefficient [$dm\,min^{-1}$]
O	Flow rate of oligomers [$g\,min^{-1}$]
O_{pores}	Flow rate of oligomers not yet solubilized [$g\,min^{-1}$]
O_{bulk}	Flow rate of oligomers solubilized in the bulk solution [$g\,min^{-1}$]
$O_{pores,ax-}$	Axial flow rate of oligomers not yet solubilized [$g\,min^{-1}$]
$O_{bulk,axial}$	Axial flow rate of oligomers solubilized in the bulk solution [$g\,min^{-1}$]
$O_{bulk,ss}$	Accumulation of oligomers in side stream [$g\,min^{-1}$]
$R_{l/s}$	Overall mass ratio of liquid to solids
SPC	Sequential plug-and-cross flow configuration
SPCC	Sequential plug-and-counter-current flow
SPCo	Sequential plug-and-co-current flow
t	Time [min]
u	Liquid velocity [$dm\,min^{-1}$]
U	Volume flow rate of the liquid [$L\,min^{-1}$]
v	Velocity of Solids [$dm\,min^{-1}$]
V_{ss}	Volume flow rate of side stream [$L\,min^{-1}$]
V	Volume flow rate of solids [$L\,min^{-1}$]
Z	Fractional progress of the liquid in the reactor [dm]

Acknowledgements

The authors are grateful for the support provided by funding grants from the Link Energy Foundation, the BioEnergy Science Center (BESC), a U.S. Department of Energy (DOE) Research Center supported by the Office of Biological and Environmental Research in the DOE Office of Science, Oak Ridge National Laboratory, and Mascoma Corporation. Oak Ridge National Laboratory is managed by University of Tennessee UT-Battelle LLC for the Department of Energy under Contract No. DE-AC05-00OR22725.

Keywords: biomass · computational chemistry · energy conversion · kinetics · renewable resources

[1] *International Energy Agency, Energy Technology Perspectives 2012: Pathways to Clean Energy System*, OECD Publishing, Paris, **2012**.
[2] M. E. Himmel, S. Y. Ding, D. K. Johnson, W. S. Adney, M. R. Nimlos, J. W. Brady, T. D. Foust, *Science* **2007**, *315*, 804 – 807.
[3] C. E. Wyman, B. Dale, R. T. Elander, M. Holtzapple, M. R. Ladisch, Y. Y. Lee, *Bioresour. Technol.* **2005**, *96*, 1959 – 1966.
[4] a) B. Yang, C. E. Wyman, *Biofuels Bioprod. Biorefin.* **2008**, *2*, 26 – 40; b) N. Mosier, C. E. Wyman, B. E. Dale, R. Elander, Y. Y. Lee, M. Holtzapple, M. Ladisch, *Bioresour. Technol.* **2005**, *96*, 673 – 686.
[5] a) B. Yang, M. C. Gray, C. Liu, T. Lloyd, S. L. Stuhler, A. O. Converse, C. E. Wyman, *ACS Symp. Ser.* **2004**, *889*, 100 – 125; b) C. Liu, C. E. Wyman, *Ind. Eng. Chem. Res.* **2004**, *43*, 2781 – 2788.
[6] a) S. G. Allen, D. Schulman, J. Lichwa, J. M. Antal, *Ind. Eng. Chem. Res.* **2001**, *40*, 2352 – 2361; b) J. A. Pérez, A. M. Gonzalez, J. M. Olivia, I. Ballesteros, P. Mansanares, *J. Chem. Technol. Biotechnol.* **2007**, *82*, 929 – 938.
[7] a) H. A. Ruiz, R. M. Rodriguez-Jasso, B. D. Fernandes, A. A. Vicente, J. A. Teixeira, *Renewable Sustainable Energy Rev.* **2013**, *21*, 35 – 51; b) A. Marcilla, A. N. Garcia, M. V. Pastor, M. Leon, A. J. Sanchez, D. M. Gomez, *Thermochim. Acta* **2013**, *564*, 24 – 33.
[8] a) C. Liu, C. E. Wyman, *Ind. Eng. Chem. Res.* **2003**, *42*, 5409 – 5416; b) Q. Yu, X. Zhuang, Z. Yuan, W. Wang, W. Qi, Q. Wang, X. Tan, *Appl. Energy* **2011**, *88*, 2472 – 2479.
[9] a) X. Shao, L. R. Lynd, *Bioresour. Technol.* **2013**, *130*, 117 – 124; b) G. Garrote, H. Dominguez, J. C. Parajo, *Process Biochem.* **2001**, *36*, 571 – 578; c) S. E. Jacobsen, C. E. Wyman, *Ind. Eng. Chem. Res.* **2002**, *41*, 1454 – 1461; d) Y. Y. Lee, Z. Wu, R. W. Torget, *Bioresour. Technol.* **2000**, *71*, 29 – 39; e) C. Pronyk, G. Mazza, *Ind. Eng. Chem. Res.* **2010**, *49*, 6367 – 6375.
[10] a) G. Bustos, J. A. Ramirez, G. Garrote, M. Vazquez, *Appl. Biochem. Biotechnol.* **2003**, *104*, 51 – 68; b) R. Aguilar, J. A. Ramirez, G. Garrote, M. Vazquez, *J. Food Eng.* **2002**, *55*, 309 – 318; c) M. A. Brennan, C. E. Wyman, *Appl. Biochem. Biotechnol.* **2004**, *115*, 965 – 976; d) Y. Lu, N. S. Mosier, *Biotechnol. Bioeng.* **2008**, *101*, 1170 – 1181; e) J. E. Morinelly, J. R. Jensen, M. Browne, T. B. Co, D. R. Shonnard, *Ind. Eng. Chem. Res.* **2009**, *48*, 9877 – 9884.
[11] J. Shen, C. E. Wyman, *Bioresour. Technol.* **2011**, *102*, 9111 – 9120.
[12] a) M. A. Brennan, Dartmouth College (Hanover), **2003**; b) S. E. Jacobsen, Dartmouth College (Hanover), **2000**.
[13] A. O. Converse, *Vol. 6632286*, Trustees of Dartmouth College, Hanover, NH, **2003**.
[14] O. Bobleter, *Prog. Polym. Sci.* **1994**, *19*, 797 – 841.
[15] C. Liu, C. E. Wyman, *Bioresour. Technol.* **2005**, *96*, 1978 – 1985.
[16] B. Marcoccia, J. R. Prough, J. Engström, J. Gullichsen in *Papermaking Science and Technology* (Ed.: J. Gullichsen and C.-J. Fogelholm), Fapet Oy, Helsinki, **2000**, pp. A512 – A570.
[17] M. H. Thomsen, A. Thygesen, A. B. Thomsen, *Bioresour. Technol.* **2008**, *99*, 4221 – 4228.
[18] K. H. Kim, M. P. Tucker, F. A. Keller, A. Aden, Q. A. Nguyen, *Appl. Biochem. Biotechnol.* **2001**, *91 – 93*, 253 – 267.
[19] F. Plaza, University of Southern Queensland (Toowoomba), **2002**.
[20] V. Archambault-Léger, X. Shao, L. R. Lynd, *Biotechnol. Biofuels* **2012**, *5*, 49.
[21] R. P. Overend, E. Chornet, *Philos. Trans. R. Soc. London Ser. A* **1987**, *321*, 523 – 536.
[22] B. Yang, C. E. Wyman, *Biotechnol. Bioeng.* **2004**, *86*, 88 – 95.
[23] V. Archambault-Léger, L. R. Lynd, *Bioresour. Technol.* **2014**, *157*, 278 – 283.
[24] M. G. Rasul, V. Rudolph, M. Carsky, *Fuel* **1999**, *78*, 905 – 910.

Received: February 21, 2014
Published online on ■■ ■■, 0000

*V. Archambault-Léger, X. Shao, L. R. Lynd**

■■ – ■■

Simulated Performance of Reactor Configurations for Hot-Water Pretreatment of Sugarcane Bagasse

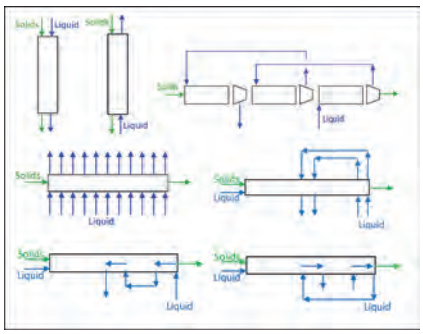

Bagasse bonus: The production of fuel from lignocellulosic biomass is of interest to develop a sustainable global energy system. Sugarcane residues such as bagasse are a particularly promising feedstock, but bagasse requires pretreatment. Simulated results show that a variety of promising flow-through pretreatment configurations result in very low sugar degradation and very high fiber digestibility for subsequent microbial or enzymatic processing to biofuel.